GEODETIC SLIP RATE ESTIMATES FOR THE KUMERING AND SEMANGKO SEGMENTS OF THE SUMATERA FAULT

Irwan Meilano[1]*, Susilo Susilo[2], Endra Gunawan [3], Budi Parjanto[2]
[1] Faculty of Earth Science and Technology, Institut Teknologi Bandung (ITB)
[2] Geospatial Information Agency, Indonesia
[3] Faculty of Mining and Petroleum Engineering, Institut Teknologi Bandung (ITB)
* *E-mail:* irwanm@itb.ac.id

Submitted: 26 August 2021 *Revised: 11 September 2021* *Accepted: 11 September 2021*

ABSTRACT

The Sumatran fault is a right lateral active inland fault in southern Sumatra, Indonesia. Although historical earthquake records have shown that magnitude 7 class earthquakes have occurred during the last century, the slip rates along the Sumatran fault have not been studied in detail. This is the first research using a new dense GPS array, in which stations are orthogonal to the fault, to analyze the fault slip rates along the Kumering and Semangko segments in southern Sumatra. In this study, we process GPS data from 14 campaign and continuous GPS points. The results show velocities of 14 mm/yr and 15 mm/yr for these two fault segments, respectively. Our geodetic slip rate estimate shows that the Sumatran fault has a relatively homogeneous slip rate from the south to the north segment, which implies that the earthquake periodization is the same along the fault.

Keywords: *Slip rate, Kumering segment, Semangko segment, Sumatran fault, GPS*

1. Introduction

In the western part of Indonesia lies the tectonically active Sunda trench, along which megathrust earthquakes have occurred during the past decade. The 4 June 2000 M7.9 and 13 February 2001 M7.3 southern Sumatra earthquakes [1], the 26 December 2004 M9.2 Sumatra-Andaman earthquake [2,3] the 28 March 2005 M8.7 Nias earthquake, the 17 July 2006 Java earthquake [4,5], the 12 September 2007 M8.5 Bengkulu earthquake [6], and the 25 October 2010 M7.8 Mentawai earthquake [7] are all examples of megathrust earthquakes caused by subduction processes between the Indo-Australia plate and Sundaland block along the Sunda trench. Apart from subduction earthquakes, this region also produces volcanic eruptions. For example, on 22 December 2018, the eruption of the Krakatau volcano produced a tsunami that killed more than 400 people.

In addition to the Sunda trench, there is a right lateral active fault inland of Sumatra named the Sumatran fault (SF). Historically, during the last century, M6.5–7 class earthquakes have occurred along the SF. The 24 June 1933 M7.5 Liwa earthquake occurred along the Kumering segment of the SF [8]. On 15 February 1994, another Liwa earthquake occurred (M6.8), causing more than 200 people to die and injuring another 200-plus. Extensive damage occurred to a long narrow zone near Liwa city [9]. The 21 January and 2 July 2013 M6.1 earthquakes occurred in the Aceh segment of the SF [10] (see Figure 1). Although the events within Sumatra Island associated with the SF are less numerous and smaller than subduction events, they may produce greatly destructive effects due to their short distance to population centers.

Previous studies have suggested that the slip rate of the SF varies from 20 mm/yr in the Aceh segment of northern Sumatra [11] to 6 mm/yr in the Kumering segment of southern Sumatra [12]. InSAR data from the ALOS-1/PALSAR-1 satellite were used to image the interseismic deformation along the SF [13]. These authors found up to ~20 mm/yr of aseismic creep on the Aceh segment along the northern SF, but no evidence from recent research of creeping in southern segment of Sumatran Fault.

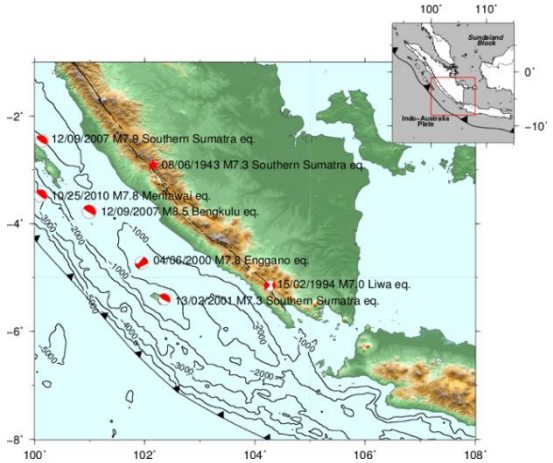

Figure 1. Tectonic setting of this research. Historical earthquakes of more than M7 in southern Sumatra. Topography drawn using SRTM (Jarvis et al., 2008); seabed contours drawn using ETOPO 1 (Amante and Eakins, 2009). Inset shows the larger regional setting.

This study uses GPS data that have not previously been published (i.e., campaign and continuous GPS observations) to analyze the slip rate in southern Sumatra. Slip rates have been analyzed for various strike faults such as the northern Dead Sea fault in northwest Syria [14] and Lembang fault in Indonesia [15] accuracy can achieve millimeter levels [16,17].

2. *Methods*

GPS Data and Processing. Campaign GPS observations in southern Sumatra conducted by the Geospatial Information Agency (BIG) of Indonesia began from early 2006 and continued until the end of 2014. Observations were carried out once a year, with a minimum observation time of 24 hours (some GPS points were observed for more than 48 hours). The total number of GPS observation points was 14. Five GPS points were located on the west side of the fault, one GPS point was right above the fault (K604), and the rest were on the east side. Because the distance from the fault line to the coastline is less than 30 km, it is difficult to install a dense GPS network on the west side of the fault. Meanwhile, continuous GPS observations began from the middle of 2008 (CTCN) and early 2009 (PALE). Figure 2 shows the locations of these campaign and continuous GPS sites in southern Sumatra.

We processed campaign and continuous GPS data using the GAMIT/GLOBK software package [18,19] We estimated the daily solutions into the International Terrestrial Reference Frame (ITRF) 2008 [20] for 20 IGS sites (ALIC, BAN2, COCO, CUSV, CNMR, DARW, DGAR, GUAM, HYDE, IISC, KARR, KOUC, LAE1, NTUS, PIMO, TOW2, TNML, WUHN, XMIS, YARR). GAMIT computes single-, double-, and triple-difference observables to correct for outliers and bias [4]. We also used standard Earth orientation parameters, precise orbits, absolute antenna phase corrections, and the FES2004 oceanic model. The final solutions generated contained the coordinates, variance and covariance matrixes, and ambiguities. Site-by-site suitable Markov a-priori North East Up condition parameters were estimated for the network adjustment with GLOBK, using the weighted root mean square of the robust fit performed. Each daily solution was weighted using the root mean square computed for repeatability. This procedure allowed for the removal of the colored noise that generally affects GNSS-permanent stations' observations [21]. GAMIT generates the solution used by GLOBK with loose constraints on parameters. Since phase ambiguities must be resolved in phase processing, GAMIT also generates several intermediate solutions with user-defined constraints before relaxing the constraints for the final solution. These steps are described in [22].

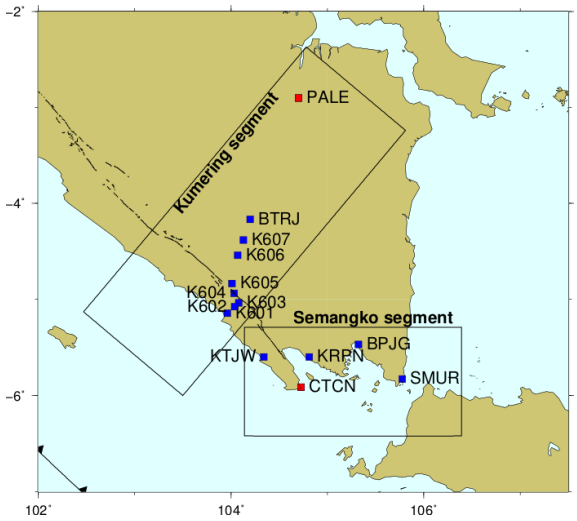

Figure 2. Location of the GPS sites used in this research. Blue and red squares imply campaign and continuous GPS observations, respectively. Each segment box contains the GPS points used to model the fault slip rates of the Kumering and Semangko segments.

3. *Results and Modeling*

During the period in which the campaign GPS data were gathered (2006–2014), the 2007 Bengkulu and 2010 Mentawai earthquakes occurred northwest of the GPS sites (Figure 1). These two earthquakes caused significant coseismic displacements, as observed by the GPS network along the west coast of Sumatra [23,24].

Unfortunately, the GPS data from our campaign GPS observations could not capture these coseismic displacements because we lacked observations just before and after the earthquake events. To carry out the analysis, based on a linear time series pattern, we thus assume that the magnitude of the postseismic deformation is very small.

To remove the coseismic displacements of the 2007 and 2010 earthquakes from the measurements at each GPS site, we first used the published coseismic slip distribution of Konca et al. [23] and Yue et al. [25]. Second, using this slip model, we calculated the surface displacements at each GPS site in southern Sumatra based on an elastic half-space model [26]. Then, we shifted the data from the GPS observations after the earthquake following the modeled coseismic displacements. Finally, after removing the coseismic displacement of the 2007 and 2010 earthquakes, we fitted the GPS data linearly. Figure 3 shows the time series of the GPS data after removing the coseismic displacements from the 2007 and 2010 earthquakes. The velocities of each GPS site in the ITRF2008 are in a southeastward direction (Figure 4).

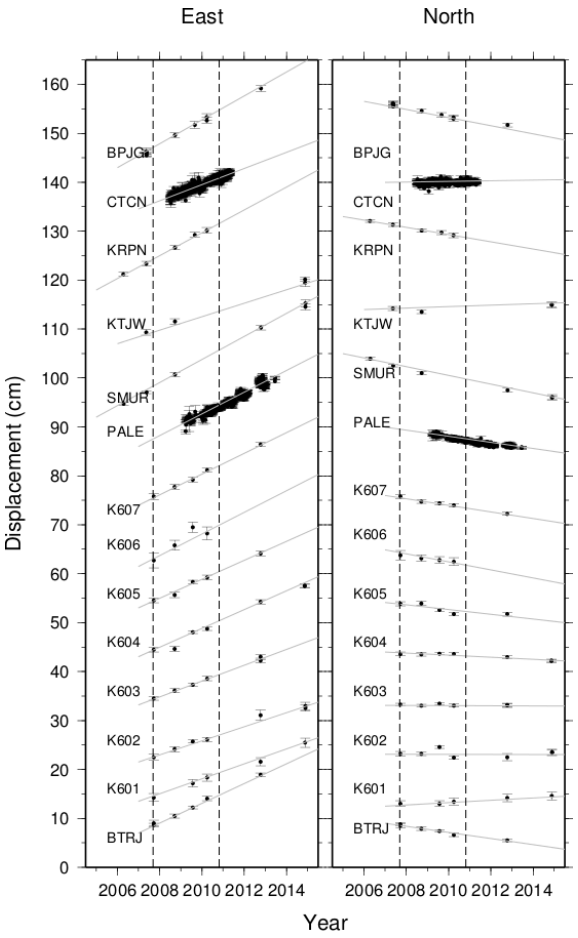

Figure 3. Time series for each GPS site in the ITRF2008 reference frame. Vertical dashed lines indicate the time of the 2007 Bengkulu and 2010 Mentawai earthquakes.

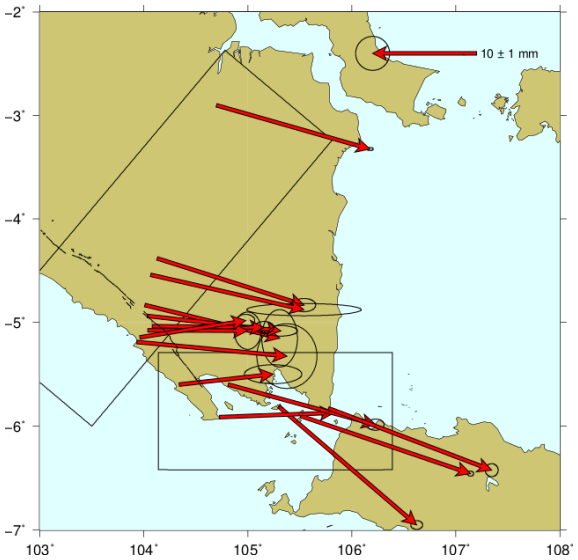

Figure 4. GPS velocities in southern Sumatra indicated by red arrows in the ITRF2008 reference

To calculate the slip rates of the Kumering and Semangko segments of the SF, we first assume the point above the fault (K604) to be a reference point to eliminate the effect of block rotation and reduce the magnitude of postseismic deformation (Figure 5).

Figure 5 shows the right-lateral (dextral) fault pattern. The observation point to the east of the fault moves toward the south-east, while the points to the west of the north-west moving fault which shows clear evidence of right-lateral motion The shift values indicate that the Semangko segment has a larger slip rate than the Semangko segment. Furthermore, the slip rate is calculated using the velocity parallel to the fault plane. We model the fault slip rates using a screw dislocation model [26,15], defined as equation 1 bellow.

$$b = V/\pi \, tan^{-1}(x/D) \qquad (1)$$

where b is the GPS site velocity, V is the slip rate, x is the distance from the fault, and D is the fault locking depth. In our case, we fix D to 16 km following the depth of the 1994 Liwa earthquake event and their aftershocks [9].

Our estimation yields fault slip rates of 14±3 mm/yr and 15±4 mm/yr for the Kumering and Semangko segments, respectively. Figure 6 shows the results of the calculation.

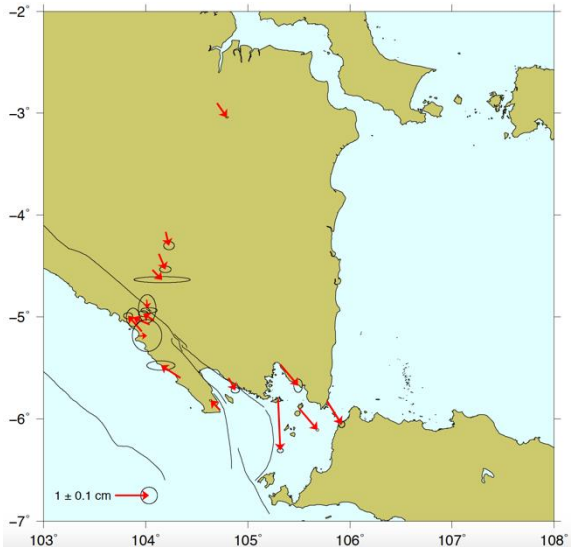

Figure 5. GPS velocities with respect to K604 located right above the fault.

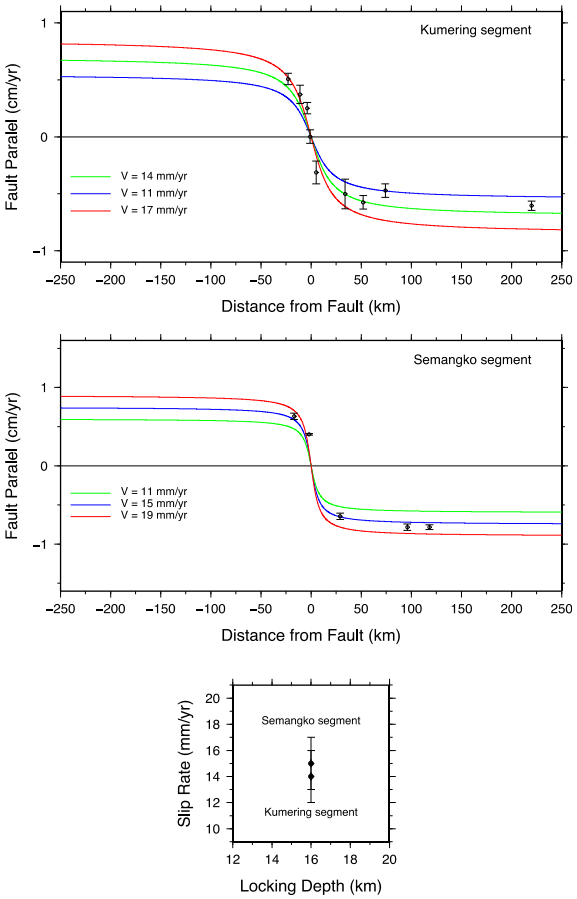

Figure 6. Slip rate calculation for (top) the Kumering segment and (middle) the Semangko segment. (Bottom) Best-fit slip rate result.

4. Discussion

We calculated the slip rates along the Kumering segment using nine GPS sites and those along the Semangko segment using five GPS sites. In total, our analysis used 14 GPS sites. Most previous research on strike slip faults has used 10 or more GPS sites to obtain better constraints for crustal deformation. For example, Lyons et al. [28] used 46 dense GPS sites to analyze the slip rate of the Imperial fault, southern California. [29] analyzed the slip rates of the northern Dead Sea fault using 36 GPS sites and [30] used 14 GPS sites to calculate the slip rates of the Husavik-Flatey fault, north Iceland. In particular, our analysis of the Semangko segment used a limited number of GPS sites. Hence, it was necessary to fix the locking depth to 16 km based on previous earthquake cases to reduce the number of unknown parameters.

Our modeled slip rate of 14 mm/yr indicates that the SF has a relatively homogeneous slip rate from 14±2 mm/yr in southern Sumatra to 20±6 mm/yr in northern Sumatra [11]. The geologic slip rate in southern Sumatra, however, has been estimated to be 11 mm/yr, lower than the geodetic result [8]. Differences in slip rates between geodetic and geologic analysis have also occurred in other tectonic regions such as in the San Andreas Fault System [31]. In the case of the slip rates of the Kumering and Semangko segments, the slip rate error from geological observations might be related to the analysis of fault planes that clustered many large earthquakes during a short period [11]. From a geodetic standpoint, the errors might be related to the underestimation of postseismic deformation from previous earthquakes.

Recent geological findings [32] show that the Semangko segment branches into two faults, one directed toward the southern region to the Sunda trench and the other directed toward the southeast. Unfortunately, using current GPS data, we cannot capture the separate contribution of each sub-segment in this region. Further research using rigid and dense GPS sites is therefore needed to map a detailed analysis of crustal deformation in this region and in other natural hazardous areas of Indonesia [33] .

5. Conclusion

This research used a new dense GPS array orthogonal to the Kumering and Semangko segments of the SF in southern Sumatra. The analysis of these segments suggests fault slip rates of 14 mm/yr and 15 mm/yr along the Kumering and Semangko segments, respectively. With reference to the results of the slip rate study in the northern part of the Sumatran fault [11],our findings indicate that the SF has relatively homogeneous slip rates between southern and northern Sumatra.

Acknowledgement. We thank two anonymous reviewers and the Editor for their thoughtful and thorough reviews.This research was partially funded by Ministry of Education, Research, Technology, and Higher Education of Indonesia No. PN-1-05-2021.

References

[1] Abercrombie, R. E., Antolik, M., and Ekström, G., The June 2000 Mw 7.9 earthquakes south of Sumatra: deformation in the India–Australia plate. Journal of Geophysical Research: Solid Earth, 108 (2003) B1. https://doi.org/10.1029/2001JB000674

[2] Gunawan, E., Sagiya, T., Ito, T., Kimata F., Tabei, T., Ohta, Y., Meilano, I., Abidin, H. Z., Agustan, Nurdin, I., and Sugiyanto, D., A comprehensive model of postseismic deformation of the 2004 Sumatra-Andaman earthquake deduced from GPS observations in northern Sumatra. Journal of Asian Earth Sciences, 88 (2014) 218–229, DOI: 10.1016/j.jseaes.2014.03.016.

[3] Anugrah, B., Meilano I., Gunawan, E., and Efendi J., Estimation of postseismic deformation parameters from continuous GPS

data in northern Sumatra after the 2004 Sumatra-Andaman earthquake. Earthquake Science, 28 (2015) 5-6, DOI: 10.1007/s11589-015-0136-x.

[4] Gunawan, E., Meilano, I., Abidin, H. Z., Hanifa, N. R., and Susilo, Investigation of the best coseismic fault model of the 2006 Java tsunami earthquake based on mechanisms of postseismic deformation. Journal of Asian Earth Sciences, 117 (2016a) 64–72, DOI: 10.1016/j.jseaes.2015.12.003.

[5] Raharja, R., Gunawan, E., Meilano, I., Abidin, H.Z. and Efendi, J., Long aseismic slip duration of the 2006 Java tsunami earthquake based on GPS data. Earthquake Science, 29(2016)5, doi: 10.1007/s11589-016-0167-y.

[6] Alif, S. M., Meilano, I., Gunawan, E., and Efendi, J., Evidence of Postseismic Deformation Signal of the 2007 M8. 5 Bengkulu Earthquake and the 2012 M8. 6 Indian Ocean Earthquake in Southern Sumatra, Indonesia, Based on GPS Data. Journal of Applied Geodesy, 10(2016) 2 , DOI: 10.1515/jag-2015-0019.

[7] Ardika, M., Meilano, I., and Gunawan, E., Postseismic deformation parameters of the 2010 M7.8 Mentawai, Indonesia, earthquake inferred from continuous GPS observations. Asian Journal of Earth Sciences, 8 (2015), DOI: 10.3923/ajes.2015.127.133.

[8] Sieh, K. and Natawidjaja, D., Neotectonics of the Sumatran fault, Indonesia. Journal of Geophysical Research: Solid Earth, 105(2000) B12, https://doi.org/10.1029/2000JB900120

[9] Widiwijayanti, C., J. Deverchere, R. Louat, H. Harjono, M. Diament, and D. Hidayat, Analysis of the aftershock sequence of the Mw 6.8 Liwa Earthquake, Indonesia, Geophys. Res. Lett., 23 (1996), https://doi.org/10.1029/96GL02048

[10] Ito, T., Gunawan, E., Kimata, F., Tabei, T., Meilano, I., Agustan, Ohta, Y., Ismail, N., Nurdin, I., Sugiyanto, D., Co-seismic offsets due to two earthquakes (Mw6.1) along the Sumatran fault system derived from GNSS measurements. Earth, Planets and Space, 68 (2016) 57, DOI: 10.1186/s40623-016-0427-z.

[11] Ito, T., Gunawan, E., Kimata, F., Tabei, T., Simons, M., Meilano, I., Agustan, Ohta, Y., Nurdin, I., and Sugiyanto, D., Isolating along-strike variations in the depth extent of shallow creep and fault locking on the northern Great Sumatran Fault. Journal of Geophysical Research: Solid Earth (1978–2012), 117 (2012) B6, DOI: 10.1029/2011JB008940.

[12] Bellier, O., and Sebrier, M., 1995. Is the slip rate variation on the Great Sumatran Fault accommodated by fore-arc stretching?. Geophysical Research Letters, 22 (1995) 15, https://doi.org/10.1029/95GL01793

[13] Tong, X., Sandwell, D.T. and Schmidt D. A., Surface creep rate and moment accumulation rate along the Aceh segment of the Sumatran fault from L-band ALOS-1/PALSAR-1 observations. Geophys. Res. Lett. , 45(2018)8, doi: 10.1002/2017GL076723

[14] Alchalbi, A., Daoud, M., Gomez, F., McClusky, S., Reilinger, R., Romeyeh, M.A., Alsouod, A., Yassminh, R., Ballani, B., Darawcheh, R. and Sbeinati, R., Crustal deformation in northwestern Arabia from GPS measurements in Syria: Slow slip rate along the northern Dead Sea Fault. Geophysical Journal International, 180(2010)1, https://doi.org/10.1111/j.1365-246X.2009.04431.x

[15] Meilano, I., Abidin, H. Z., Andreas, H., Gumilar, I., Harjono, H., Kato, T., Kimata, F., and Fukuda, Y., Slip rate estimation of the Lembang Fault West Java from geodetic observation., Journal of Disaster Research, 7(2012)1, doi: 10.20965/ jdr. 2012.p0012

[16] Ohkura, T., Tabei, T., Kimata, F., Bacolcol, T. C., Nakamura, Y., Luis, A. C., Pelicano, A., Jorgio, R., Tabique, M., Abrahan, M., Jorgio, E., and Gunawan, E., Plate Convergence and Block Motions in Mindanao Island, Philippine as Derived from Campaign GPS Observations., Journal of Disaster Research, 10(2015)1, doi: 10.20965/jdr.2015.p0059

[17] Gunawan, E., Kholil, M., and Meilano, I.,. Splay-fault rupture during the 2014 Mw7. 1 Molucca Sea, Indonesia, earthquake determined from GPS measurements. Physics of the Earth and Planetary Interiors, 259 (2016b), DOI: 10.1016/j.pepi.2016.08.009.

[18] Herring, T. A., King, R. W., and McClusky, S. C., GAMIT Reference Manual Release 10.4, report, 1–171, Massachusetts Institute Technology, Cambridge (2010a).

[19] Herring, T. A., King, R. W., and McClusky, S. C., 2010b. GLOBK Reference Manual: Global Kalman filter VLBI and GPS analysis program, Release 10.4, report, 1–95, Massachusetts Institute Technology, Cambridge (2010b).

[20] Altamimi, Z., Collilieux, X., and Métivier, L., ITRF2008: an improved solution of the international terrestrial reference frame. Journal of Geodesy, 85(2011)8, https://doi.org/10.1007/s00190-011-0444-4

[21] Casula, G., Geodynamics of the Calabrian Arc area (Italy) inferred from a dense GNSS network observations, Geodesy and Geodynamics, 7(2016)1, https://doi.org/ 10.1016/ j.geog.2016.01.001

[22] Herring, T.A., King, R.W., Floyd, M.A., McClusky, S.C. GAMIT Reference Maunal 10.6. In Proceedings of the GAMIT–GPS Analysis at MIT (2015), Department of Earth, Atmospheric, and Planetary Sciences

Massachusetts Institute of Technology: Cambridge, MA, USA.
[23] Konca, A. O., Avouac J.P., Sladen A., Meltzner A. J., Sieh K., Fang P., Li Z., Galetzka J., Genrich J., Chlieh M., Natawidjaja D. H., Bock Y., Fielding E. J., Ji C., and Don V., Helmberger D. V., Partial rupture of a locked patch of the Sumatra megathrust during the 2007 earthquake sequence, Nature, 456 (2008), doi:10.1038/nature07572.
[24] Hill E. M., Borrero J. C., Huang Z., Qiu Q., Banerjee P., Natawidjaja D H., Elosegui P., Fritz H. M., Suwargadi B.W., Pranantyo I. R., Li L. L., Macpherson K. A., Skanavis V., Synolakis C. E., Sieh K., The 2010 Mw 7.8 Mentawai earthquake: Very shallow source of a rare tsunami earthquake determined from tsunami field survey and near-field GPS data, Journal of Geophysical Research:, 117 (2012) B06402, https://doi.org/ 10.1029/2012JB009159
[25] Yue H., Lay T., Rivera L., Bai Y., Yamazaki Y.,Cheung K. F., Hill E. M., Sieh K., Kongko W., Muhari A., Rupture process of the 2010 Mw 7.8 Mentawai tsunami earthquake from joint inversion of near-field hr-GPS and teleseismic body wave recordings constrained by tsunami observations , Journal of Geophysical Research: Solid Earth, 119(2014)7 , https://doi.org/10.1002/2014JB011082
[26] Okada Y., Internal deformation due to shear and tensile faults in a half-space, Bulletin of the Seismological Society of America , 82 (1992) 2, 1018-1040.
[27] Savage, J.C. and Burford, R.O., Geodetic Determination of Relative Plate Motion in Central California. Journal of Geophysical Research, 78 (1973) http://dx.doi.org/ 10.1029/ JB078i005p00832
[28] Lyons, S. N., Bock, Y., and Sandwell, D. T., Creep along the Imperial Fault, southern California, from GPS measurements. Journal of Geophysical Research: Solid Earth, 107 (2002) B10., https://doi.org/10.1029/2001JB000763
[29] Alchalbi, A., Daoud, M., Gomez, F., McClusky, S., Reilinger, R., Romeyeh, M.A., Alsouod, A., Yassminh, R., Ballani, B., Darawcheh, R. and Sbeinati, R., Crustal deformation in northwestern Arabia from GPS measurements in Syria: Slow slip rate along the northern Dead Sea Fault. Geophysical Journal International, 180(2010)1, https://doi.org/10.1111/j.1365-246X.2009.04431.x
[30] Metzger, S., Jónsson, S. and Geirsson, H., Locking depth and slip-rate of the Húsavík Flatey fault, North Iceland, derived from continuous GPS data 2006-2010. Geophysical Journal International, 187(2011) 2, https://doi.org/10.1111/j.1365-246X.2011.05176.x
[31] Tong, X., Sandwell, D.T. and Smith-Konter, B., High-resolution interseismic velocity data along the San Andreas fault from GPS and InSAR. Journal of Geophysical Research: Solid Earth, 118(2013)1, https://doi.org/10.1029/2012JB009442
[32] Natawidjaja, D.H., Updating Active Fault Data of Indonesia. The 3rd International Conference on Earthquake Engineering and Disaster Mitigation Bali, Indonesia, 2016
[33] Gunawan, E., Ghozalba, F., Syauqi, Widiastomo, Y., Meilano, I., Hanifa, N. R., Daryono, and Hidayati, S., Field Investigation of the November to December 2015 Earthquake Swarm in West Halmahera, Indonesia. Geotechnical and Geological Engineering, 35(2017)1, 425-432, DOI: 10.1007/s10706-016-0117-4.